JOURNAL OF AGRICULTURAL AND FOOD CHEMISTRY

Effect of Ethanol, Temperature, and Gas Flow Rate on Volatile Release from Aqueous Solutions under Dynamic Headspace Dilution Conditions

MAROUSSA TSACHAKI,*,† ANNE-LAURE GADY,†,‡ MICHALIS KALOPESAS,† ROBERT S. T. LINFORTH,† VIOLAINE ATHÈS,‡ MICHELE MARIN,‡ AND ANDREW J. TAYLOR†

Samworth Flavor Laboratory, Division of Food Sciences, School of Biosciences, University of Nottingham, Sutton Bonington Campus, Loughborough LE12 5RD, United Kingdom, and UMR 782 Génie et Microbiologie des Procédés Alimentaires, AgroParisTech, INRA, F-78850 Thiverval Grignon, France

On the basis of a mechanistic model, the overall and liquid mass transfer coefficients of aroma compounds were estimated during aroma release when an inert gas diluted the static headspace over simple ethanol/water solutions (ethanol concentration = 120 mL·L^{-1}). Studied for a range of 17 compounds, they were both increased in the ethanol/water solution compared to the water solution, showing a better mass transfer due to the presence of ethanol, additively to partition coefficient variation. Thermal imaging results showed differences in convection of the two systems (water and ethanol/water) arguing for ethanol convection enhancement inside the liquid. The effect of ethanol in the solution on mass transfer coefficients at different temperatures was minor. On the contrary, at different headspace dilution rates, the effect of ethanol in the solution helped to maintain the volatile headspace concentration close to equilibrium concentration, when the headspace was replenished 1−3 times per minute.

KEYWORDS: Real-time APCI-MS; ethanol; modeling; mass transfer coefficient; thermal imaging; Marangoni effect

INTRODUCTION

The underlying principle governing aroma release from a liquid into the gas phase is the partition coefficient (*1*). It describes the distribution of a volatile compound between a liquid and the gas phase at equilibrium, and it is expressed by the following equation:

$$K_{al} = \frac{C_g}{C_l} \quad (1)$$

where K_{al} is the air/liquid partition coefficient and C_g and C_l are the concentrations of the volatile compound in the gas and liquid phase, respectively.

Various properties of the volatile compound and the nature of the liquid determine the value of K_{al} (molecular size, functional groups, shape, vapor pressure, and hydrophobicity of the molecule, etc). The air/liquid partition coefficient is also temperature dependent. The log transformed K_{al} is linearly related to the temperature (*2*).

The most studied combination is an air/water system, and values of the air/water partition coefficient (K_{aw}) for a wide range of volatile compounds can be found scattered in the literature or can be calculated from Henry's law constant values found in several databases (*3*). There are several methods for determining air/water partition coefficients; however, often enough results show discrepancies, and there is lack of agreement between different methods (*3, 4*). This is more important for volatiles with very low and very high values of K_{aw} (*5*).

The partition of volatiles between air and other solutions has been determined such as an air/oil or air/water−ethanol system. Ethanol in the liquid acts as a cosolvent with water and affects the solubility of the volatile fraction of the solution. A decrease in the partition coefficient of volatiles of 30−35% was observed when the ethanol concentration of the solution was increased from 5 to 80 mL·L^{-1} (*6*). However, in other studies, a decrease in the infinite dilution activity coefficients of volatiles has only been observed at ethanol solution concentrations above 170 mL·L^{-1} (*7*).

Under nonequilibrium conditions, which are the majority in real life, the driving force for mass transfer of volatile molecules from one phase to the other is the difference in the concentration of the volatile compounds in the two phases. The rate of mass transfer from the liquid to the gas phase depends on the

* To whom correspondence should be addressed. Fax: +30 28210 40507. E-mail: maroussat@gmail.com.
† University of Nottingham.
‡ INRA.

10.1021/jf800225y CCC: $40.75
Published on Web 06/05/2008

concentration gradient and the mass transfer coefficient of the volatile compounds in each of the phases.

Two main mechanisms for volatile transport have been suggested for food matrices in general, which are applicable in liquid systems as well.

The first mechanism is diffusion, and it is based on the fact that mass transport occurs because of random Brownian movement of molecules within a stagnant fluid, creating a concentration gradient from the interface to the bottom of the phase. In a given phase, the diffusivity varies only slightly between volatile compounds, and it is found in the range of 10^{-5} and 10^{-9} $m^2 \cdot s^{-1}$ in gas and aqueous phases, respectively (*2*).

The second mechanism is convection. In this case, it is assumed that the phases are well mixed by either natural convection or forced convection (agitation of the fluids). Mass transport across the interface occurs by diffusion in very thin layers (boundary layers) on either side of the interface. At the interface, an instantaneous equilibrium is assumed, and the concentration of the volatile at both sides of the interface is given by the partition coefficient. In the gas phase, a uniform concentration of volatile compounds is assumed, again because of inevitable convection. Convective mass transfer characteristic of the gas phase is related to the Reynold's number, and an increase of mass transfer is observed from laminar to turbulent flow (*8*).

The overall mass transport across the interface can be described by the following equation (*8*):

$$\frac{1}{k} = \frac{1}{k_g} + \frac{K_{al}}{k_l} \quad (2)$$

where k is the overall mass transfer coefficient referred to the concentration difference expressed in the gas phase and k_g and k_l are the mass transfer coefficients in the gas and liquid phase, respectively.

On the basis of the above mechanisms, several mathematical models have been presented to describe the dynamic release of flavors both from a solution (or a food matrix in general) to the gas phase and in-mouth (*3, 9, 10*). Marin et al. (*8*) have specifically studied and modeled the gas phase volatile concentration when an inert gas diluted the equilibrium headspace (dynamic headspace analysis), on the basis of mass transfer (eq 2) and mass balance in each phase (air and liquid). As a result, the exploitation of the model validated with the first sets of experimental data allows defining the main limiting mechanisms during dilution in headspace. For volatile compounds with low K_{aw} values (below 10^{-5}), in a simple air/water system, $1/k_g \gg K_{aw}/k_l$, and therefore, the driving force of the overall mass transfer was the mass transfer in the gas phase, expressed by k_g. For those molecules, the equilibrium headspace concentration was not depleted upon dilution. On the contrary, for volatiles with higher K_{aw} values, K_{aw}/k_l became a significant factor, and the mass transfer was basically affected by the K_{aw} value. For those molecules, the equilibrium headspace concentration depleted readily upon dilution.

However, in an air/water−ethanol system, other physical mechanisms may enhance the overall mass transfer coefficient, due to the ethanol. In previous studies, it was shown that the presence of ethanol helped to maintain the volatile headspace concentration when the ethanol solution concentration was above 50 $mL \cdot L^{-1}$ (*11*). This effect was such that, under dynamic conditions, the absolute volatile concentration above an ethanol/water solution was higher than that above an aqueous solution, contrary to results observed in equilibrium studies. The ratio of the headspace concentration of volatiles above ethanol/water (ethanol 120 $mL \cdot L^{-1}$) and water solutions was correlated to their air/water partition coefficient. However, the air/water partition coefficient alone is not expected to significantly affect the dynamic aroma release from a water−ethanol solution, as at least an order of magnitude in the K_{al} values was needed in other studies to observe a change in dynamic aroma release profiles (*12*).

The interfacial properties of ethanol in water, like other alcohols, seem to affect the properties of the interfacial boundary layer and therefore change the overall mass transfer of the system. Ethanol is surface active, and in water-ethanol solutions, it places itself preferentially at the air/liquid interface, lowering the surface tension (*13, 14*) at all alcohol concentrations (*15, 16*). A characteristic phenomenon observed in water−ethanol solutions, which is the direct result of the interfacial properties of ethanol, is the so-called Marangoni effect or Marangoni convection (*17–19*). The Marangoni effect denotes the carrying of bulk material to the interface through motions energized by surface tension gradients. Therefore, the driving force for mass transfer in this case is the differences in the surface tension at the surface. These differences may occur from temperature or concentration changes. Therefore, the ability of volatile compounds to maintain their headspace concentration under dynamic conditions above water−ethanol solutions was related to convection in the solution (*11*) and therefore to an increase in the overall mass transfer in the system.

In the present work, the origins of this increase in the overall mass transfer will be investigated. To study the overall mass transfer and the mass transfer in the liquid, the dynamic headspace concentration data produced by Tsachaki et al. (*11*) were fitted to a physical model of mass transfer. The kinetic parameters (the overall mass transfer coefficient and liquid mass transfer coefficient) generated by the model were studied. Moreover, the effect of temperature and headspace dilution rates on the mass transfer coefficients was investigated.

MATERIALS AND METHODS

Chemicals. Acetaldehyde, propanal, 2-butanol, diacetyl, 3-methyl-1-butanol, furfuryl alcohol, *c*-3-hexenol, ethyl-2-butenoate, phenylacetaldehyde, octanal, ethyl isovalerate, *p*-cymene, eucalyptol (1,8-cineole), and linalool were purchased from Sigma-Aldrich (Poole, U.K.); ethyl butyrate and (+)-limonene were obtained from Acros (Loughborough, U.K.); 1-octen-3-one was from Lancaster (Morecambe, England); and terpinolene from Fluka (Poole, U.K.). Ethanol (analytical reagent grade, 99.99%) was purchased from Fisher Scientific (Loughborough, U.K.). All volatile compounds were of 97% purity or greater apart from terpinolene and phenylacetaldehyde, which were of 90% purity.

Atmospheric Chemical Ionization Mass-Spectrometry (APCI-MS). Data for the static and dynamic headspace concentration of volatile compounds were obtained from Aznar et al. (*20*) and Tsachaki et al. (*11*), apart from data at different headspace dilution rates and temperatures, which took place as described below.

A platform LCZ mass spectrometer was used and fitted with an MS Nose interface (Micromass, Manchester, U.K.) to sample the headspace above the solutions. The APCI source was operated with a modification, as described previously (*20*), such that ethanol was added to the nitrogen makeup gas in the range 2.0−11.3 $\mu L \cdot L^{-1}$, depending on the ethanol concentration of the sample. This was done to ensure that the final concentration of ethanol in the source was the same whatever the ethanol concentration of the sample.

Individual solutions of the volatile compounds tested were prepared in water in the following concentration ranges: propanal, 70−75 $\mu L \cdot L^{-1}$; ethyl-2-butenoate, 1.0−1.5 $\mu L \cdot L^{-1}$; *p*-cymene, 0.5−1.0 $\mu L \cdot L^{-1}$; eucalyptol, 4.0−4.5 $\mu L \cdot L^{-1}$; ethyl butyrate, 1.5−2.0 $\mu L \cdot L^{-1}$; and 1-octen-3-one, 4.0−4.5 $\mu L \cdot L^{-1}$. These solutions were then diluted

Table 1. Air/Liquid Partition Coefficients of Volatiles for Aqueous Solution (K_{aw}) and Ethanol Solution (120 mL·L^{-1}, K_{aa})[a]

volatile	K_{aw}[b]	K_{aa}[c]	k water (m·s^{-1})	k ethanolic solution (m·s^{-1})
cis-3-hexenol	3.35×10^{-5}	2.87×10^{-5}	2.70×10^{-2}	5.00×10^{-2}
furfuryl alcohol	3.65×10^{-5}	3.47×10^{-5}	3.50×10^{-2}	3.00×10^{-2}
2-butanol	4.17×10^{-5}	4.11×10^{-5}	3.70×10^{-3}	6.70×10^{-3}
phenylacetaldehyde	3.93×10^{-4}	2.71×10^{-4}	4.50×10^{-2}	4.30×10^{-2}
3-methylbutanol	5.77×10^{-4}	3.27×10^{-4}	4.60×10^{-3}	1.20×10^{-2}
linalool	8.25×10^{-4}	5.56×10^{-4}	2.20×10^{-2}	2.90×10^{-2}
eucalyptol	1.10×10^{-3}	7.65×10^{-4}	6.70×10^{-4}	5.40×10^{-2}
diacetyl	1.32×10^{-3}	1.35×10^{-3}	4.60×10^{-3}	1.10×10^{-2}
ethyl 2-butenoate	1.68×10^{-3}	1.34×10^{-3}	6.40×10^{-4}	1.10×10^{-2}
propanal	1.70×10^{-3}	1.58×10^{-3}	3.60×10^{-4}	7.20×10^{-3}
1-octen-3-one	3.13×10^{-3}	2.09×10^{-3}	8.50×10^{-4}	1.90×10^{-2}
ethyl butyrate	9.56×10^{-3}	7.74×10^{-3}	2.10×10^{-4}	4.70×10^{-3}
ethyl isovalerate	1.05×10^{-2}	8.06×10^{-3}	5.70×10^{-5}	1.40×10^{-3}
octanal	2.54×10^{-2}	1.42×10^{-2}	1.10×10^{-4}	1.20×10^{-3}
limonene	2.73×10^{-2}	2.98×10^{-2}	3.20×10^{-5}	1.10×10^{-4}
terpinolene	3.84×10^{-2}	2.63×10^{-2}	4.03×10^{-5}	7.60×10^{-5}
p-cymene	1.04×10^{-1}	1.16×10^{-1}	4.03×10^{-5}	1.50×10^{-4}

[a] The overall mass transfer coefficient (k) extracted from the model for aqueous and ethanolic (120 mL·L^{-1}) solutions. [b] Taken from Tsachaki et al. (*11*). [c] Determined from K_{aw} values and experimental static headspace concentration values from Tsachaki et al. (*11*).

with water or ethanol to make the final water or ethanolic solutions, respectively. The volume of water and ethanol used was such that, for each individual volatile compound, its final solution concentration was the same in both. For static headspace studies, the volatile solution (40 mL) was placed in 123 mL flasks (Sigma-Aldrich, Poole, U.K.) fitted with a one-port lid. After equilibration for at least two hours at ambient temperature (22 °C), unless otherwise stated, headspace was sampled through the port into the APCI-MS with a sample flow rate of 5 mL·min^{-1}. The sample entered the APCI-MS through a heated (140 °C) deactivated fused silica transfer line, which minimized any losses or absorption of volatiles. The concentration used for each volatile was within the infinite dilution range (*3*). Static headspace studies have also taken place at different solution temperatures: 7, 15, 22, 26, and 37 °C. During these studies, a dilution device (dilution 1:400) was used to dilute the sample gas flow with nitrogen just before the sample entered the mass spectrometer sampling line, to minimize the effect of ethanol on the ionization of volatile compounds.

For dynamic headspace studies, volatile solutions (100 mL) were placed in 123 mL flasks fitted with a two-port lid. After equilibration, N_2 was introduced through one port to dilute the headspace. As the gas flowed out of the second port, part of the gas flow was sampled into the mass spectrometer (5 mL·min^{-1}) for 10 min. To study the effect of different dilution rates, different headspace dilution rates were used: 15 mL·min^{-1} (replenishment of headspace 0.65 times per minute), 30 mL·min^{-1} (replenishment of headspace 1.3 times per minute), 50 mL·min^{-1} (replenishment of headspace 2.2 times per minute), and 70 mL·min^{-1} (replenishment of headspace 3 times per minute). The profiles were normalized to the signal intensity at the start of the time course (100%). Statistical analysis was performed with SPSS 12.0.1 for Windows, SPSS Inc. 1-Octen-3-one, propanal, and ethyl butyrate were studied. For the effect of different temperatures, dynamic headspace concentration analyses were performed with a headspace dilution rate of 70 mL·min^{-1} after equilibration for at least 2 h in water baths at 7, 22, and 37 °C. Samples were kept in the water baths at the specific temperature throughout the 10 min of the experiment. A dilution device (dilution 1:400) was used as described above for static headspace studies.

Partition Coefficient. Values of the air/water partition coefficient (K_{aw}) were taken from Tsachaki et al. (*11*). The air/ethanolic solution partition coefficient (K_{aa}) was calculated from K_{aw} and the relative change in the headspace concentration of volatiles when ethanol was present in the solution, taken from Tsachaki et al. (*11*). The values of K_{aw} and K_{aa} are presented in **Table 1**.

Modeling. The equations of the model (*8*) were incorporated into a program written in Matlab 7.0.4 (The MathWorks Inc.). The kinetic parameters (mass transfer coefficients) extracted were the ones minimizing the sums of squared differences between each experimental point and its corresponding modeled point. The common input parameters for all the volatiles used for the mathematical model were as follows: the volume of the liquid phase was 100 mL (1×10^{-4} m^3); the volume of the gas phase was set at 50 mL (5×10^{-5} m^3), which included the part of the flask not filled with liquid and some space left between the flask and the lid; the gas flow rate was 70 mL·min^{-1} (1.17×10^{-6} m^3·s^{-1}), unless otherwise stated; and the area of interface was measured by measuring the internal diameter of the flask at the point of the liquid surface (1×10^{-3} m^2).

Thermal Imaging Analysis. An Agema Thermovision 900 (Agema Infrared Systems, Sweden; currently Flir Systems, Boston, MA) thermal imaging camera was used (wavelength range 8−12 μm, mercury−cadmium−telluride detector). Two flasks were used, made of Duran borosilicate glass that is an opaque material to IR radiation (*21*), and were filled up to the top with liquid. They were placed next to each other and 45 cm below the thermal imaging camera. The thermal imaging camera was set to store images (Erika software, Agema, Sweden) at an interval of 30 s for the duration of 7 min (total of 15 images). The sequence was started with a manual keyboard trigger. An air stream was generated parallel to the surface of the two flasks by a fan at a distance of 0.7 m (air flow of 2.06×10^{-5} m^3·s^{-1}). The first image was taken at 0 s when no air stream was generated, and directly after the storage of the first image, the air stream was turned on and stayed on until the end of the image storage sequence. All the solutions tested and flasks used were kept in a water bath (set at 20 °C) prior to the experiment for at least 2 h to ensure uniformity of the temperature of the samples and with the room temperature.

RESULTS AND DISCUSSION

The ability of volatiles above ethanolic solutions to maintain their headspace concentration under dynamic dilution conditions has been related to the increase in overall mass transfer in the system. This could be associated with convective forces created in the liquid (Marangoni convection) due to the presence of ethanol.

Data from Tsachaki et al. (*11*) were modeled using equations that describe the behavior of volatiles in headspace during gas phase dilution (*8*). Data from the dynamic headspace analysis of volatiles above aqueous and ethanolic solutions had a reasonable fit to the model, to a greater or lesser extent depending on the volatile. For some molecules, such as ethyl butyrate and octanal (**Figure 1**), the model was able to predict quite accurately the aroma release profile. For other molecules, such as eucalyptol and 1-octen-3-one, the model could predict the aroma release less accurately (**Figure 1**). It seemed that, in the latter cases, the model was able to predict the dynamic aroma release above ethanolic solutions better than above water solutions (**Figure 1**; eucalyptol, 1-octen-3-one). This might have

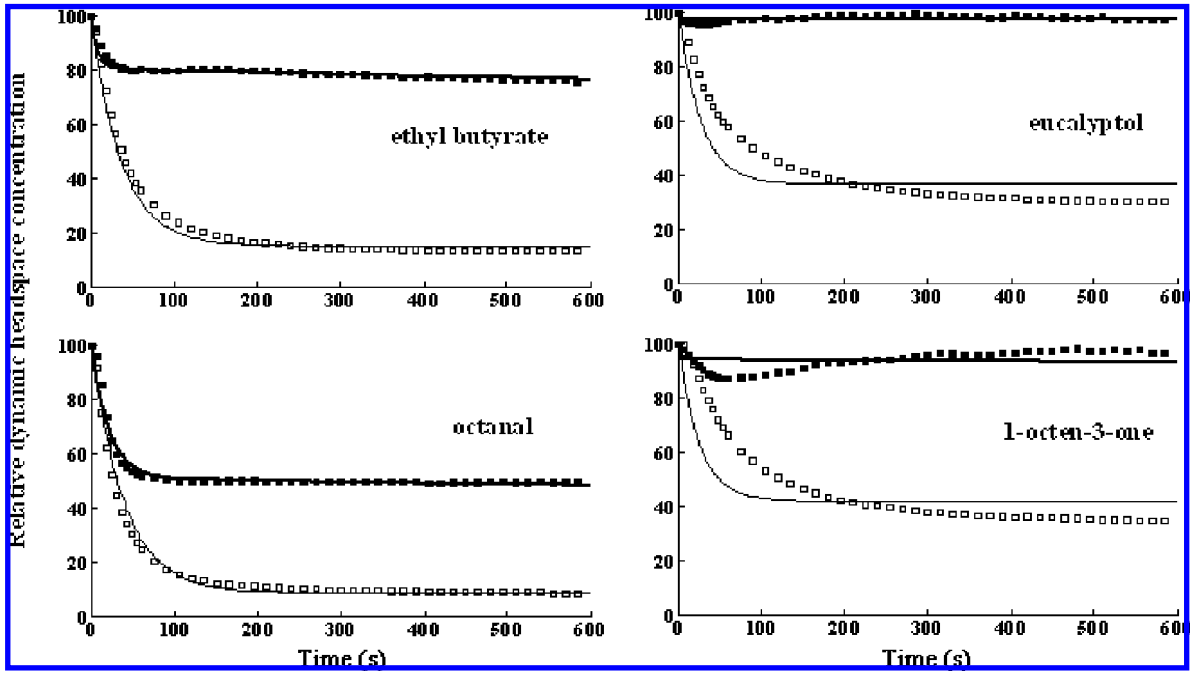

Figure 1. Relative dynamic headspace concentration profile (%) of four volatiles above aqueous solution (□, experimental; −, predicted from the model) and ethanolic solution (120 mL·L^{-1}; ■, experimental; −, predicted from the model) as an inert gas diluted the equilibrium headspace.

been an artifact from the fact that, in the majority of cases, the relative steady-state concentration above an ethanolic solution was much closer to 100% of the initial concentration. Therefore, the error observed seemed less, contrary to the real situation. On the other hand, as the relative steady concentration above water solutions was further away from 100% of the relative concentration, the error seemed greater. Alternatively, the difference in the shape of the eucalyptol and ethyl butyrate curves may indicate further factors not included in the current model of volatile behavior in solution.

The fit between the model and the experimental findings was achieved by changing the value of k, the overall mass transfer coefficient (**Table 1**). In this model, three main parameters contribute to the overall mass transfer coefficient: the mass transfer from the bulk liquid to the interface, expressed by the liquid mass transfer coefficient (k_l); the equilibrium partitioning of the volatile, expressed by the air/liquid partition coefficient (K_{al}); and the gas phase mass transfer coefficient (k_g).

The overall process is described by eq 2. The values for the overall mass transfer coefficient (k) were extracted from the model. They were greater for the majority of volatile molecules for 120 mL·L^{-1} ethanolic solution compared to those for aqueous solution (**Table 1**). A range of increases in k was observed from 2- to 80-fold. For some compounds, such as furfuryl alcohol and phenyl acetaldehyde, k was of the same order of magnitude in water and in ethanolic solution (**Table 1**). However, for these compounds, k was already very high, and there may have been a limited potential for ethanol to increase the mass transfer.

According to eq 2, in order to get this increase in k for ethanolic solutions (120 mL·L^{-1}) compared to aqueous solutions, there must be a change in one of the parameters K_{al}, k_g, or k_l. Given the equation, we can attempt to determine which factors are the main ones that have changed, driving the differences in volatile release into the headspace and consequently resistance of the headspace volatile concentration to dilution.

Effect of k_g. The mass transfer coefficient in the gas phase, k_g, is dependent on the experimental conditions (volume of gas phase, air flow rate, and temperature). Those remained the same when analyzing both aqueous and ethanolic solutions. In previous studies, an experimental value of k_g was calculated (3.0×10^{-2} m·s^{-1}) for the volatiles tested (*8*). Further studies showed both experimental and theoretical values were similar and very close to 3.0×10^{-2} m·s^{-1} for all volatiles tested (*12*). The experiments described in the current study were performed under virtually identical experimental conditions to the earlier studies. Therefore, this value of k_g would be used in the model, assuming nonsignificant variations in the value of k_g in all cases.

For the compounds in **Table 1** with a quite low K_{aw} (lower than 10^{-3}), such as *cis*-3-hexenol, furfuryl alcohol, 2-butanol, phenylacetaldehyde, 3-methyl butanol, and linalool, k_g was the main parameter affecting the overall mass transfer coefficient (*8*). The low partition coefficient values for these compounds resulted in a value of $1/k_g$ much greater than that of K_{al}/k_l (*8*). Consequently, their overall mass transfer coefficients were virtually identical for both ethanolic systems and water. For the rest of the molecules, with higher K_{aw}, k_g has a lower impact on the overall mass transfer ($1/k_g \ll K_{al}/k_l$), and k was mainly determined by the term K_{al}/k_l. These showed the greatest differences in k between the ethanolic solutions and water.

Effect of K_{al} on Mass Transfer of the System. K_{al} is one parameter that can be measured directly. The values in **Table 1** show that the air/liquid partition coefficients for ethanolic solutions were lower than those for water alone and lower partition coefficients would decrease K_{al}/k_l and hence increase k. However, the difference between K_{aw} and K_{aa} was less than a factor of 2. This would be considered unlikely to account for the magnitude of the changes in headspace behavior observed (**Figure 1**).

An average value for k_l of 2.4×10^{-6} m·s^{-1} was obtained for the water solutions of compounds, where $K_{aw}/k_l \gg 1/k_g$ using the values of k for water and K_{aw} from **Table 1** with a k_g of 3×10^{-2} m·s^{-1}. The value for k_l was very similar to values of k_l previously reported by Marin et al. (*8*). When the value for k_l obtained for water was used along with K_{aa} and a k_g of 3×10^{-2} m·s^{-1} to predict the value of k for ethanolic solutions (using eq 2), the majority of the values of k for the ethanolic

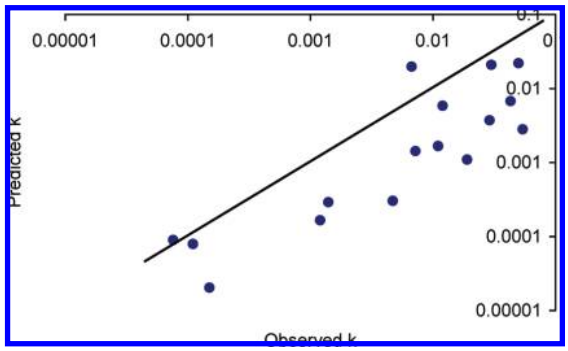

Figure 2. Predicted vs observed overall mass transfer coefficient (k in $m \cdot s^{-1}$) for ethanolic solutions. The predicted k was based on K_{aa} (**Table 1**), a k_g of 3×10^{-2} $m \cdot s^{-1}$, and a k_l of 2.4×10^{-6} $m \cdot s^{-1}$. The trend line shows the line for the correlation $x = y$.

Table 2. Liquid Mass Transfer Coefficient (k_l) and Ratio of K_{al}/k_l in Aqueous and Ethanolic (120 $mL \cdot L^{-1}$) Solutions[a]

	k_l ($m \cdot s^{-1}$)		K_{al}/k_l	
volatile	aqueous solution	ethanolic solution (120 $mL \cdot L^{-1}$)	aqueous solution	ethanolic solution (120 $mL \cdot L^{-1}$)
2-butanol	1.76×10^{-7}	3.55×10^{-7}	237	116
diacetyl	7.17×10^{-6}	2.34×10^{-5}	184	58
ethyl 2-butenoate	1.10×10^{-6}	2.33×10^{-5}	1529	58
propanal	6.19×10^{-7}	1.50×10^{-5}	2744	106
ethyl butyrate	2.02×10^{-6}	4.31×10^{-5}	4729	179
ethyl isovalerate	6.00×10^{-7}	1.18×10^{-5}	17511	681
octanal	2.80×10^{-6}	1.78×10^{-5}	9058	800
limonene	8.75×10^{-7}	3.29×10^{-6}	31217	9058
terpinolene	1.55×10^{-6}	2.00×10^{-6}	24781	13125
p-cymene	4.20×10^{-6}	1.75×10^{-5}	24781	6633

[a] Values of k_l calculated from eq 1 with K_{al} values taken from **Table 1** and k_g set at 3.0×10^{-2} $m \cdot s^{-1}$.

system was not well predicted (**Figure 2**). The majority of the predictions was under estimates and fell bellow the $x = y$ line denoting a perfect correlation. Consequently, the differences in k between the ethanolic and water solutions were greater than expected on the basis of changes in K_{al} alone. This implies that there were also changes in the mass transfer in the liquid phase. By substituting k_g, k, and K_{aa} into eq 2 it was possible to determine values of k_l for the ethanolic system.

Effect of k_l. Marin et al. (*8*) suggested that in their system the mass transfer coefficient in the liquid (k_l) remained the same for all volatile compounds. k_l represents mass transfer in the liquid phase. In ethanolic solutions, bulk convection in the liquid could be more pronounced because of the Marangoni convection (*11*), so k_l in our system was expected to have a significant effect on the values of the overall mass transfer coefficient. The changes in K_{al} were not sufficient to cause the changes in the dynamic aroma release of volatiles (**Figure 2**).

Values of k_l were extracted from the model, for molecules where $1/k_g \ll K_{al}/k_l$. For those molecules, k_l increased by almost a factor of 2 (terpinolene) to a factor of 25 (propanal) when ethanol was present in the solution (**Table 2**). This increase in k_l would significantly affect the value of the overall mass transfer coefficient, much greater than changes in K_{al} alone.

To show more clearly the effect that the increase in k_l could have on the overall mass transfer coefficient, the ratio of K_{al}/k_l was calculated for some volatile compounds (**Table 2**). For these molecules, the reciprocal of the overall mass transfer is directly reflected to the ratio of K_{al}/k_l, as k_g is less significant. Consequently, the lower the value of K_{al}/k_l, the higher the value of k. Therefore, it seems that mass transfer in the liquid phase (k_l) was the main driver for the ability of volatiles to maintain their headspace concentration under dynamic conditions.

Thermal Imaging Analysis. To further investigate the above hypothesis, thermal images of the surface of simple water/ethanol solutions were studied. A thermal image arises from temperature variations or differences in emissivity within a scene. All objects are composed of continually vibrating atoms with higher energy atoms vibrating more frequently. The higher the temperature of an object, the faster the vibration, and thus the higher the spectral radiant energy. As a result, all objects above absolute zero are repeatedly emitting radiation at a rate and with a wavelength distribution that depends upon the temperature of the object and its spectral emissivity (*22*).

Control measurements of empty flasks showed a reasonably uniform pink color against an orange background (**Figure 3**, **panel I**). This was due to the so-called Narcissus effect formed by the reflected energy from the surrounding objects and the IR camera itself on the flask (*21, 23*). This was also the case for the IR images of the ethanol and water samples (**Figure 3**, **panel II**) in the region outside the dotted circle. The darker blue color on the region of the flask walls, just outside the dotted circle, was due to evaporation of traces of liquid left on them.

The surface temperature of the water solution dropped with time (**Figure 3**, **panel II**, **b**). However, the surface temperature of the ethanolic solution (120 $mL \cdot L^{-1}$) remained the same throughout the experiment, showing a completely different behavior from water. The lower latent heat of vaporization of ethanol (latent heat of vaporization of water = 2540 $kJ \cdot kg^{-1}$ at 20 °C; latent heat of vaporization of ethanol = 1045 $kJ \cdot kg^{-1}$ at 20 °C (*24*)) should result in faster evaporation of the ethanol/water mixture, which would lead to an evaporative cooling on the liquid surface. However, the ethanol (120 $mL \cdot L^{-1}$) solution surface temperature did not change throughout the duration of the experiment (450 s), contrary to the results expected.

This was attributed to the convective forces in the liquid (Marangoni effect), which were able to replenish the surface with bulk solution. In this way, the ethanolic solution was able to keep the temperature of the interface constant throughout the experiment. For the water solution, the absence of bulk convective forces resulted in a drop in the surface temperature with time due to evaporative cooling.

Effect of Headspace Dilution Rate on Mass Transfer in Ethanolic Solutions. Lower headspace dilution rates should lead to higher steady-state volatile concentrations during dynamic headspace analysis, as the molecules that are leaving the system for a given unit of time are fewer, principally, through changes in k_g. This was the case for volatile concentration profiles above aqueous solutions (**Table 3**). The steady-state relative headspace concentration of 1-octen-3-one during dynamic studies at a headspace dilution rate of 15 $mL \cdot min^{-1}$ above water solution was 49% of the initial concentration (**Figure 4**, **panel A**; **Table 3**). This decreased to 20% of the initial concentration when a headspace dilution rate of 70 $mL \cdot min^{-1}$ was used. The final, relative steady-state concentration of the volatiles above the water solutions decreased exponentially with the increase in headspace dilution rate (**Table 3**).

At a headspace dilution rate of 15 $mL \cdot min^{-1}$, the steady-state relative concentration for all volatiles was virtually identical for the aqueous and ethanolic solutions (**Table 3**), suggesting the same system behavior and mass transfer coefficients. As the dilution gas flow rate increased, the steady-state headspace concentration increased and stabilized. Consequently, the steady-state headspace concentration of the volatiles above the ethanolic

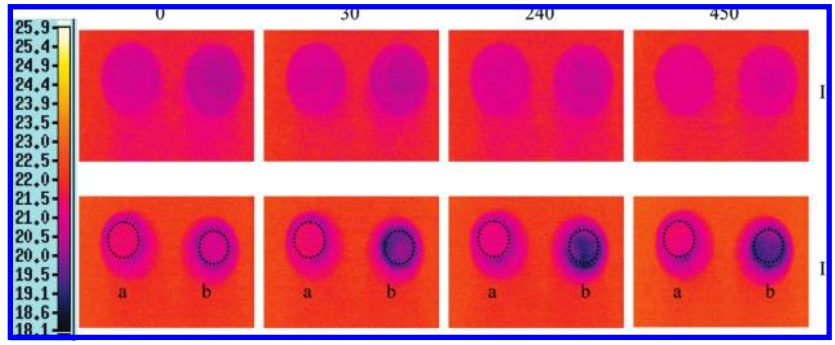

Figure 3. Thermal images: (**Panel I**) top of empty flasks (volume 123 mL); (**Panel II**, **a**) top of ethanol solution 120 mL·L^{-1} in flask (volume 123 mL); (**Panel II**, **b**) top of water solution in flask (volume 123 mL) at 0, 30, 240, and 450 s of air flow blowing at 2.06 × 10^{-5} m^3·s^{-1}·1.24 × 10^{-3} m^3·min^{-1} parallel to the surface of the liquid from a distance of 0.7 m. Dotted circles denote the surface area of the liquid.

Table 3. Relative Dynamic Volatile Headspace Concentration (DHS) at the End of the Dilution Process for Different Headspace Dilution Rates[a] and Overall Mass Transfer Coefficient (*k*) of Volatiles at Different Headspace Dilution Rates in Aqueous and Ethanol (120 mL·L^{-1}) Solutions, Extracted from the Model[b]

	ethyl 2-butenoate		eucalyptol		1-octen-3-one	
flow rate (mL·L^{-1})	DHS (%)	*k* (m·s^{-1})	DHS (%)	*k* (m·s^{-1})	DHS (%)	*k* (m·s^{-1})
			aqueous solution			
15	55^{c} (±7)	4.60 × 10^{-4}	60^{c} (±8)	5.43 × 10^{-4}	49^{c} (±6)	4.85 × 10^{-4}
30	41^{d} (±2)	6.78 × 10^{-4}	40^{d} (±2)	6.78 × 10^{-4}	30^{d} (±2)	4.72 × 10^{-4}
50	33^{d,e} (±2)	8.79 × 10^{-4}	34^{d,e} (±1)	7.79 × 10^{-4}	24^{d,e} (±1)	6.23 × 10^{-4}
70	26^{e} (±1)	1.00 × 10^{-3}	28^{e} (±1)	1.00 × 10^{-3}	20^{e} (±1)	4.40 × 10^{-3}
			ethanolic solution (120 mL·L^{-1})			
15	60^{c} (±4)	3.70 × 10^{-4}	59^{c} (±4)	3.80 × 10^{-4}	54^{c} (±4)	3.00 × 10^{-4}
30	78^{d} (±4)	1.68 × 10^{-3}	83^{d} (±1)	2.26 × 10^{-3}	78^{d} (±1)	1.76 × 10^{-3}
50	78^{d} (±2)	3.39 × 10^{-3}	85^{d} (±3)	4.97 × 10^{-3}	80^{d} (±6)	3.82 × 10^{-3}
70	74^{d} (±4)	1.59 × 10^{-2}	83^{d} (±10)	7.26 × 10^{-2}	74^{d} (±7)	3.63 × 10^{-2}

[a] Each value is the average of three replicates; numbers in parentheses represent the standard deviation of the mean. [b] Different letters for each volatile/same solution denote significant differences at 0.05 level.

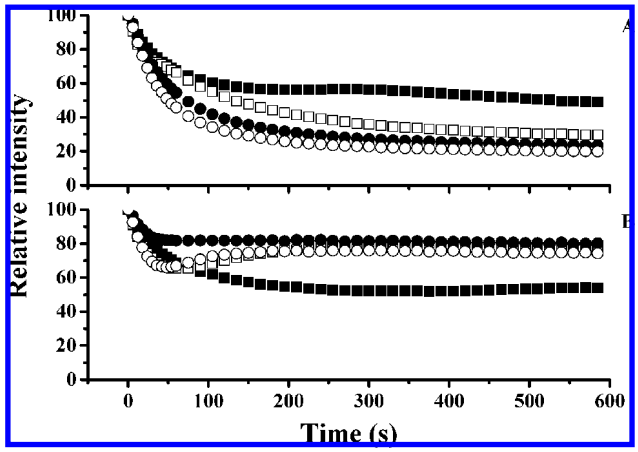

Figure 4. Relative dynamic headspace concentration profile of 1-octen-3-one above water (**A**) and 120 mL·L^{-1} ethanol solution (**B**) as an inert gas diluted the headspace at different dilution rates (■, 15 mL·min^{-1}; □, 30 mL·min^{-1}; ●, 50 mL·min^{-1}; ○, 70 mL·min^{-1}). Each point is the mean of three replicates. The percentage coefficient of variation was less than 9% for each point.

solution at headspace dilution rates of 30 and 50 mL·min^{-1} was not significantly different to the steady-state headspace concentration of the volatiles at a headspace dilution rate of 70 mL·min^{-1} ($p > 0.05$; **Table 3**).

The overall mass transfer coefficient increased for three of the molecules tested both above aqueous and ethanol (120 mL·L^{-1}) solutions with the increase in headspace dilution rate, reflecting greater volatile loss from the system with increased gas flow. For aqueous solutions, *k* increased by a factor of 2−9, whereas *k* in ethanol solutions (120 mL·L^{-1}) increased by a factor of 40−200. Changes in k_g should be broadly similar for the two systems as the gas flow rate was varied. Equally, K_{al} would be the same at all gas flow rates for each solution. Therefore, the relative difference in *k* between the aqueous and ethanolic solutions as the dilution rate changed would depend on changes in k_l.

At 15 mL·min^{-1}, there were only minor differences between the two systems, implying that any Marangoni effects were minimal. As the flow increased, the changes in the mass transfer were consistent with an increase in convection enhancing mass transfer and delivering volatiles to the interface. In combination with the thermal imaging results, this strongly suggests that ethanol evaporation from the surface at 15 mL·min^{-1} was insufficient to induce ethanolic streaming and replenish interfacial volatile concentrations. With increasing gas flows, the greater evaporation caused more bulk streaming of ethanol carrying volatiles to the surface, increasing k_l.

The net effect of the changes in *k* was that the presence of ethanol in a solution can minimize the effect of gas phase dilution rate on aroma release. In other words, in cases such as during the tasting of an alcoholic beverage and wine (sniffing, stirring of the glass, etc) differences in the headspace dilution rate, which always occur, would be less significant (except for cases of very low headspace dilution rates).

Effect of Temperature on Ethanol Partitioning. The method used to study the static and dynamic aroma release from ethanolic solutions was based on a constant delivery of ethanol in the APCI-MS source (*20*) and its use as the reagent ion. However, changes in solution temperature were expected to have an important effect on the amount of ethanol delivered in the system from the sample and to significantly affect the static and dynamic headspace profiles of volatiles. Therefore, the

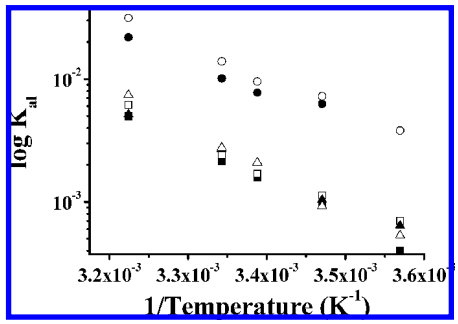

Figure 5. Air/liquid partition coefficient, K_{al}, of volatiles as a function of temperature. Propanal in water □, or 120 mL·L^{-1} ethanol ■; ethyl butyrate in water, ○ or 120 mL·L^{-1} ethanol ●; 1-octen-3-one in water △, or 120 mL·L^{-1} ethanol ▲.

concentration of ethanol in the headspace was studied at different temperatures to investigate if the APCI-MS method could be used reliably at different solution temperatures.

The ethanol concentration in the headspace above ethanolic solutions was found to vary substantially with temperature. Increasing the temperature of the solution from 7 to 37 °C resulted in a more than 200% fold increase in the headspace ethanol concentration. This difference could substantially affect the ionization process of volatiles during both static and dynamic headspace analysis. Therefore, a dilution device (dilution 1:400) was used for the headspace analysis of volatiles to dilute the sample flow with nitrogen just before the sample entered the APCI-MS sampling line. This was done to keep the ethanol concentration within the detection limits of the APCI-MS for all the samples at different temperatures and to avoid any changes in ionization of the volatiles due to the differences in ethanol source concentration.

Effect of Temperature on Aroma Partitioning. An effect of temperature on K_{al} is expected, since any constants of equilibrium are linked to the standard free energy of the reaction ($\Delta_r G^0$, in joules per mole) and to the temperature (T, in Kelvin) by Arhenius law:

$$K_{al}(T) = \exp\left(-\frac{\Delta_r G^0}{RT}\right) \quad (3)$$

with R, the Universal gas constant (8.3145 J·mol^{-1}·K^{-1}).

$\Delta_r G^0$ is a function of the attractions and repulsions of a molecule with other molecules (same molecules and solvent molecules) in a solution. As a result, the air/liquid partition coefficient is a function of the aroma compound, the solution, and the temperature of the experiment. If the reaction is endothermic ($\Delta_r G^0 > 0$), K_{al} will increase with the temperature. On the contrary, if the reaction is exothermic ($\Delta_r G^0 < 0$), K_{al} will decrease with temperature.

The air/liquid partition coefficient of the three volatiles tested decreased exponentially ($R^2 > 0.975$) versus the inverse of temperature (Kelvin), as expected from eq 3, (**Figure 5**). From eq 3, the values of the free energy of reaction can be calculated, which were between 50.2 and 63.3 kJ·mol^{-1} for the three volatiles tested in both the solutions (water, 120 mL·L^{-1} ethanol). These experimental values of the Gibb's enthalpy for the reaction were in agreement with the range of values, around 50 kJ·mol^{-1}, found in the literature (*25*). Since $\Delta_r G^0$ was positive, the reaction was endothermic, and K_{al} increased with an increase in temperature. The Gibb's enthalpy of reaction was roughly equivalent in aqueous and in ethanolic (120 mL·L^{-1}) solutions; thus, the increase of the partition coefficient with an increase of temperature was similar for both water and ethanolic (120 mL·L^{-1}) solutions. Therefore, the decrease in K_{al} follows the same trend for both solutions (**Figure 5**). K_{al} was approximately 10-fold lower for the 7 °C solutions compared with the 37 °C solutions, such that the change in partitioning behavior with temperature was much greater than that caused by adding ethanol (120 mL·L^{-1}) to the system.

Effect of Temperature on Dynamic Headspace Behavior. Under dynamic conditions, the aqueous system might be expected to show differences caused by the changes in K_{al} or the effect of temperature on k_g and k_l, reflecting changes in convection, diffusion, viscosity, and density. In the case of the ethanolic solutions, the change in temperature may affect the capacity of the system to establish evaporative streaming induced convection and hence mass transfer due to changes in the rate of ethanol volatilization. Consequently, the dynamic headspace behavior of the two systems might become more similar at temperatures lower than 22 °C and accentuated at higher temperatures.

The effects of temperature on dynamic headspace behavior were much less than the effects of dilution gas flow rate. The relative headspace concentration at the end of the dilution process under dynamic conditions above ethanol solutions (120 mL·L^{-1}) did not show significant differences at different temperatures (**Table 4**). On the contrary, for aqueous solutions, the general trend was a significant decrease of the relative steady-state headspace concentration of volatiles with the increase in temperature (**Table 4**).

Although the magnitude of the differences in volatile behavior between the aqueous and ethanolic systems decreased overall as the temperature decreased, there were clearly still considerable

Table 4. Air/Liquid Partition Coefficients above Aqueous (K_{aw}) and Ethanolic (120 mL·L^{-1}, K_{aa}) Solutions, Relative Headspace Concentration of Volatiles at the End of the Dynamic Headspace Analysis (DHS), Liquid Mass Transfer Coefficient (k_l), and Ratio of Air/Liquid Partition Coefficient to Liquid Mass Transfer Coefficient (K_{al}/k_l) under Dynamic Release Conditions for Volatiles at Different Temperatures[a]

		aqueous solution			ethanolic solution (120 mL·L^{-1})		
	T (°C)	DHS (%)	K_{aw}	K_l (m·s^{-1})	DHS (%)	K_{aa}	K_l (m·s^{-1})
propanal	7	67[b] (±2)	7.00×10^{-4}	2.80×10^{-6}	88[b] (±5)	4.00×10^{-4}	4.80×10^{-6}
	22	51[c] (±10)	1.70×10^{-3}	3.50×10^{-6}	90[b] (±8)	1.60×10^{-3}	2.20×10^{-5}
	37	51[c] (±9)	6.20×10^{-3}	2.60×10^{-5}	90[b] (±9)	5.00×10^{-3}	nd
ethyl butyrate	7	32[b] (±4)	3.80×10^{-3}	5.40×10^{-6}	78[b] (±1)	3.80×10^{-3}	4.80×10^{-5}
	22	26[b] (±7)	9.60×10^{-3}	1.30×10^{-5}	74[b] (±11)	7.70×10^{-3}	5.20×10^{-5}
	37	21[b] (±3)	3.10×10^{-2}	1.10×10^{-5}	66[b] (±11)	2.20×10^{-2}	1.20×10^{-4}
1-octen-3-one	7	72[b] (±6)	8.00×10^{-3}	4.20×10^{-4}	92[b] (±6)	6.40×10^{-4}	1.63×10^{-5}
	22	34[c] (±7)	3.10×10^{-2}	1.30×10^{-4}	78[c] (±5)	2.10×10^{-3}	9.60×10^{-6}
	37	26[c] (±6)	1.10×10^{-1}	8.50×10^{-5}	82[b,c] (±10)	5.10×10^{-3}	8.35×10^{-5}

[a] DHS values at 7 and 37 °C are average of three replicates and at 22 °C are average of six replicates; values in parentheses represent the standard deviation of the mean. Different letters for each volatile/same solution denote significant difference at the 0.05 level.

differences in volatile behavior between the two systems at 7 °C. This strongly suggests that, even at 7 °C, ethanol evaporation can induce streaming in the liquid phase that minimizes the depletion of volatile flavor compounds at the interface.

In conclusion, mass transfer in the liquid phase was the main parameter affected by the presence of ethanol enhancing flavor delivery and maintaining higher headspace volatile concentrations than those seen for aqueous solutions. The increased mass transfer of the liquid phase is caused by ethanol streaming rather than cooling induced convection. This occurs if there is sufficient gas flow to affect the ethanolic interface. This process can occur in ethanolic systems at a range of temperatures, which is again consistent with ethanolic streaming rather than cooling induced convection.

ABBREVIATIONS USED

K, Overall mass transfer coefficient; k_l, mass transfer coefficient in the liquid phase; k_g, mass transfer coefficient in the gas phase; K_{al}, air/liquid partition coefficient, when referring to any kind of liquid; K_{aw}, air/water partition coefficient; K_{aa}, air/ethanolic solution partition coefficient; IR, infra-red; $\Delta_r G^0$, standard free energy of the reaction; T, temperature; R, Universal gas constant.

ACKNOWLEDGMENT

Innovative Research Centre, University of Nottingham, for the thermal imaging camera.

LITERATURE CITED

(1) Taylor, A. J. Physical chemistry of flavour. *Int. J. Food Sci. Technol.* **1998**, *33*, 53–62.
(2) van Ruth, S. M.; Roozen, J. P. Delivery of flavours from food matrices. In *Food Flavour Technology*; Taylor, A. J., Ed.; Sheffield Academic Press: Sheffield, U.K., 2002; pp 167−184.
(3) Taylor, A. J. Release and transport of flavors in vivo: physicochemical, physiological and perceptual considerations. *Compr. Rev. Food Sci. Food Saf.* **2002**, *1*, 45–57.
(4) Athes, V.; Lillo, M. P. Y.; Bernard, C.; Perez-Correa, R.; Souchon, I. Comparison of experimental methods for measuring infinite dilution volatilities of aroma compounds in water/ethanol mixtures. *J. Agric. Food Chem.* **2004**, *52*, 2021–2027.
(5) Tsachaki, M. Factors Determing Aroma Release from Wine-based Systems. Ph.D. Thesis, University of Nottingham, Nottingham, U.K., 2006.
(6) Fischer, C.; Fischer, U.; Jacob, L. *Impact of Matrix Variables Ethanol, Sugar, Glycerol, pH and Temperature on the Partition Coefficients of Aroma Compounds in Wine and Their Kinetics of Volatilization*, Proceedings for the 4th International Symposium on Cool Climate Viticulture and Enology, Rochester, NY, July 16−20, 1996; Henick-Kling, T., Wolf, T. E., Harkness, E. M., Eds.; New York State Agricultural Experiment Station: Geneva, NY, 1996; pp 42−46.
(7) Conner, J. M.; Birkmyre, L.; Paterson, A.; Piggott, J. R. Headspace concentrations of ethyl esters at different alcoholic strengths. *J. Sci. Food Agric.* **1998**, *77* (1), 121–126.
(8) Marin, M.; Baek, I.; Taylor, A. J. Volatile release from aqueous solutions under dynamic headspace dilution conditions. *J. Agric. Food Chem.* **1999**, *47*, 4750–4755.
(9) deRoos, K. B. Physicochemical models of flavor release from foods. In *Flavor Release*; Roberts, D. D., Taylor, A. J., Eds.; Americal Chemical Society: Washington, DC, 2000; pp 166−178.
(10) Linforth, R. S. T.; Friel, E.; Taylor, A. J. Modelling aroma release from foods using physicochemical parameters. *Abstr. Pap. Am. Chem. Soc.* **1999**, *218*, 71–AGFD..
(11) Tsachaki, M.; Linforth, R. S. T.; Taylor, A. J. Dynamic headspace analysis of the release of volatile organic compounds from ethanolic systems by direct APCI-MS. *J. Agric. Food Chem.* **2005**, *53*, 8328–8333.
(12) Doyen, K.; Carey, M.; Linforth, R. S. T.; Marin, M.; Taylor, A. J. Volatile release from an emulsion: Headspace and in-mouth studies. *J. Agric. Food Chem.* **2001**, *49*, 804–810.
(13) Guggenheim, E. A.; Adam, N. K. The thermodynamics of adsorption at the surface of solutions. *Proc. R. Soc. London, Ser. A* **1933**, *139* (837), 218–236.
(14) Li, Z. X.; Lu, J. R.; Styrkas, D. A.; Thomas, R. K.; Rennie, A. R.; Penfold, J. The structure of the surface of ethanol-water mixtures. *Mol. Phys.* **1993**, *80*, 925–939.
(15) Nishi, N.; Takahashi, S.; Matsumoto, M.; Tanaka, A.; Muraya, K.; Takamuku, T.; Yamaguchi, T. Hydrogen-bonded cluster formation and hydrophobic solute association in aqueous solutions of ethanol. *J. Phys. Chem.* **1995**, *99*, 462–468.
(16) Stewart, E.; Shields, R. L.; Taylor, R. S. Molecular dynamics simulations of the liquid/vapor interface of aqueous ethanol solutions as a function of concentration. *J. Phys. Chem. B* **2003**, *107*, 2333–2343.
(17) Marangoni, C. On the expansion of a drop of liquid floating on the surface of another liquid. Ph.D. Thesis, University of Pavia, Pavia, Italy, 1865.
(18) Hosoi, A. E.; Bush, J. W. M. Evaporative instabilities in climbing films. *J. Fluid Mech.* **2001**, *442*, 217–239.
(19) Molenkamp, T. Marangoni convection, Mass Transfer and Microcravity. Ph.D. Thesis, Universiteit Groningen, Groningen, The Netherlands, 1998.
(20) Aznar, M.; Tsachaki, M.; Linforth, R. S. T.; Ferreira, V.; Taylor, A. J. Headspace analysis of volatile organic compounds from ethanolic systems by direct APCI-MS. *Int. J. Mass Spectrom.* **2004**, *239*, 17–25.
(21) Buffone, C.; Sefiane, K. IR measurements of interfacial temperature during phase chance in a confirmed environment. *Exp. Therm. Fluid Sci.* **2004**, *29* (1), 65–74.
(22) Rogalski, A.; Chrzanowski, K. Infrared devices and techniques. *Opto-Electron. Rev.* **2002**, *10* (2), 111–136.
(23) Horny, N. FPA camera standardisation. *Infrared Phys. Technol.* **2003**, *44* (2), 109–119.
(24) Perry, R. H.; Green, D. W. *Perry's Chemical Engineers' Handbook*; McGraw-Hill: New York, 1984.
(25) Meynier, A.; Garillon, A.; Lethuaut, L.; Genot, C. Partition of five aroma compounds between air and skim milk, anhydrous milk fat or full-fat cream. *Lait* **2003**, *83* (3), 223–235.

Received for review January 22, 2008. Revised manuscript received April 2, 2008. Accepted April 12, 2008. Greek State Scholarship Foundation (IKY) for financial support to M.T.

JF800225Y